International Journal of
Mathematical Modelling & Computations
Vol. 05, No. 02, Spring 2015, 99- 109

Tension Quartic Trigonometric Bézier Curves Preserving Interpolation Curves Shape

A. Lamnii[a,*], F. Oumellal [a] and J. Dabounou[a]

[a] *Faculty of Sciences and Technology, University Hassan first, Settat, Morocco.*

Abstract. In this paper simple quartic trigonometric polynomial blending functions, with a tension parameter, are presented. These type of functions are useful for constructing trigonometric Bézier curves and surfaces, they can be applied to construct continuous shape preserving interpolation spline curves with shape parameters. To better visualize objects and graphics a tension parameter is included. In this work we constructed the Trigonometric Bézier curves followed by a construction of the shape preserving interpolation spline curves with local shape parameters and finally several numerical examples are presented such as open shape preserving interpolation curve, closed shape preserving interpolation curve and surfaces. As a direct application we computed the area surrounded by a closed curve.

Received: 1 March 2014, Revised: 12 May 2014, Accepted: 23 August 2014.

Keywords: Trigonometric Bézier Curves, Tension Parameter, Shape Parameter, Interpolation,

Index to information contained in this paper

1. Introduction

In recent years, several new spline curve and surface schemes have been proposed for geometric modeling in Computer Aided Geometric Design (CAGD). Recently, in order to overcome the limitations of the Non-Uniform Rational B-Splines (NURBS) methods in the applications of CAGD, important studies have been done using different trigonometric polynomial to represent diverse curves and surfaces [9, 19]. In the area of shape-preserving interpolation for planar curve, considerable progress has been made by several authors (see [11, 18, 20]). Particular attention has been paid to study shape preserving interpolation which has been a subject of great

*Corresponding author. Email: a_lamnii@yahoo.fr

http://www.ijm2c.ir

interest in CAGD. Many papers have dealt with alternative techniques for shape representation (see [9, 17, 18, 20] for a review of these techniques). Basing on Bernstein basis, Kui [11] and Kui and Xingming [12] gave a kind of shape preserving interpolation curves, respectively. Zhu et al. [20] reported recently new quartic trigonometric polynomial blending functions. Lamnii et al. [15], presented an alogorithm of decomposition and reconstruction corresponding to the 2π-periodic algebraic trigonometric wavelets and discussed their applications in the area of approximation of planar closed curves.

Polynomial B-spline curves have been widely used on the grounds of flexibility and efficiency. In order to improve the shape of a curve and adjust the extent which a curve approaches its control polygon, some methods of generating curve were presented by using tension parameters, see [9, 19]. Constructing curves and surfaces, which preserve the shape implied by the data, has been extensively studied by several authors [7, 16, 17].

It is important to study the spline curve representations that provide local control, that is, the capability of modifying one portion of the curve without altering the remainder. From a practical standpoint, we are interested in constructing the trigonometric polynomial representations which can manipulate a curve effectually. The purpose of this paper is to present quartic trigonometric polynomial blending functions where we include a tension parameter β, the latter is mainly important for object visualization. These blending functions are useful for constructing trigonometric Bézier curves and can be applied to construct continuous shape preserving interpolation spline curves with shape parameters. Using tensor product, we can construct Bézier-type surfaces, which have properties similar to polynomial Bézier surfaces.

The remainder of this paper is organized as follows. In section 2, the quartic Trigonometric polynomial blending functions are described and the properties of these functions are shown. In the same section, Trigonometric Bézier curves are constructed. Trigonometric parametric curve segments are illustrated in section 3. The Trigonometric polynomial interpolation is discussed in Section 4. In section 5, several numerical examples are presented in which open and closed Trigonometric curves as well as area of closed planar curves are described. Conclusion is given in section 6.

2. Trigonometric Bézier Curves

With the basis defined in [20], we can define the generalized quartic trigonometric polynomial blending functions with tension parameter β and the corresponding generalized trigonometric Bézier curves.

2.1 *Quartic Trigonometric Polynomial Blending Functions with Tension parameter β*

The quartic trigonometric polynomial blending functions proposed in this section are quite similar to those introduced by ZHU et al. in [20].

Definition 2.1 *Let β be the tension parameter and $t \in [0, \frac{\pi}{2\beta}]$. The generalized Quartic trigonometric polynomial blending functions with tension parameter*

$B_{i,\beta},\ i = 0, ..., 5$ *are defined as:*

$$\begin{cases} B_{0,\beta}(t) = (1 - \sin(\beta t))^4, \\ B_{1,\beta}(t) = 4\sin(\beta t)(1 - \sin(\beta t))^3, \\ B_{2,\beta}(t) = (1 - \sin(\beta t))^2(1 - \cos(\beta t))(9 + 8\sin(\beta t) + 3\cos(\beta t)), \\ B_{3,\beta}(t) = (1 - \sin(\beta t))(1 - \cos(\beta t))^2(9 + 3\sin(\beta t) + 8\cos(\beta t)), \\ B_{4,\beta}(t) = 4\cos(\beta t)(1 - \cos(\beta t))^3, \\ B_{0,\beta}(t) = (1 - \cos(\beta t))^4. \end{cases} \tag{1}$$

Figure 1, plots these basis functions for different values of the tension parameter β in the interval $[0, \frac{\pi}{2\beta}]$.

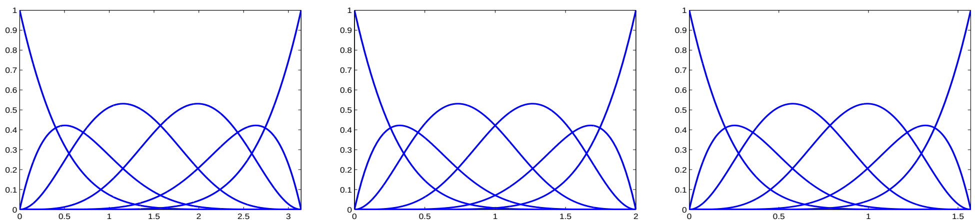

(a) $\beta = 0.5$. (b) $\beta = \pi/4$. (c) $\beta = 1$.

Figure 1. The curves of the blending functions basis (for $t \in [0, \frac{\pi}{2\beta}]$).

The blending functions studied in the present work have the following properties which are analogous to those found for the quintic trigonometric Bézier basis functions (see [20]):

(1) Nonnegativity : $\forall t \in [0, \frac{\pi}{2\beta}],\ B_{i,\beta}(t) \geqslant 0,\ i = 0, ..., 5$.

(2) Partition of unity : $\sum_{i=0}^{5} B_{i,\beta}(t) = 1$.

(3) Symmetry : $B_{i,\beta}(t) = B_{5-i,\beta}(\frac{\pi}{2\beta} - t)$, for $i = 0, 1, 2$.

(4) Maximum : Each $B_{i,\beta}$ has one maximum value in $[0, \frac{\pi}{2\beta}]$.

2.2 *Trigonometric Bézier Curves with Tension Parameter*

This section describes the theory and method of using the tension parameter β to control the form of the interpolating trigonometric Bézier curve $B_\beta(t)$. Note that changing the tension factor β does not affect the form of $B_\beta(t)$ and the interpolation features at the data points.

Let $V = \{V_0, ..., V_5\}$ be a set of points $V_i \in \mathbb{R}^2$ or $\mathbb{R}^3$. The Trigonometric Bézier curves with tension parameter $\beta > 0$ associated with the set V is defined by:

$$B_\beta(t) = \sum_{i=0}^{5} B_{i,\beta}(t) V_i, \qquad t \in [0, \frac{\pi}{2\beta}]. \tag{2}$$

The points $V_i,\ (i = 0, ..., 5)$ are called quartic trigonometric Bézier control points.

Figure 1 shows the quartic Trigonometric Bézier curves with different tension parameter values. Keeping the same control polygon, as β varies we are not simply changing the domain of a single curve, but defining different curves. It can be seen that quartic trigonometric Bézier curves are close to the control polygon. Therefore, quartic trigonometric Bézier curves can nicely preserve the feature of the control polygon. Control polygons provide an important tool in geometric modeling. The tension-like effect of this tension factor β is illustrated in Figures 1 and 2 where the interval changes as a function of β keeping all the properties of the blending functions verified. It is an advantage if the curve being modeled tends to preserve the shape of its control polygon.

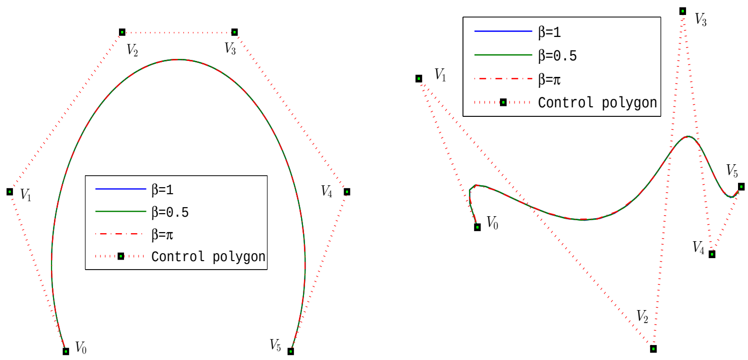

Figure 2. The curves of the blending functions basis (for $t \in [0, \frac{\pi}{2\beta}]$).

We find the important geometric properties analogous to those of the Bézier curves and those described in [20], so that we can write:

(1) Terminal properties: straightforward computation, we have:

$$\begin{cases} B_\beta(0) = V_0, \\ B'_\beta(0) = 4(V_1 - V_0)\beta, \\ B''_\beta(0) = 12(V_0 - 2V_1 + V_2)\beta^2, \\ B_\beta(\frac{\pi}{2\beta}) = V_5, \\ B'_\beta(\frac{\pi}{2\beta}) = 4(V_5 - V_4)\beta, \\ B''_\beta(\frac{\pi}{2\beta}) = 12(V_3 - 2V_4 + V_5)\beta^2. \end{cases} \tag{3}$$

(2) Trigonometric Bézier curves exhibit a symmetry property : $V_0, ..., V_5$ and $V_5, ..., V_0$ define the same trigonometric Bézier curve, i.e., $B_\beta(t; V_0, V_1, V_2, V_3, V_4, V_5) = B_\beta(\frac{\pi}{2\beta} - t, V_5, V_4, V_3, V_2, V_1)$.

(3) Geometric invariance: since the blending functions have the properties of partition of unity, the shape of these trigonometric Bézier curves is independent of the choice of coordinates.

(4) Convex hull property: the blending functions have the properties of nonnegativity and partition of unity, as a consequence, the trigonometric Bézier curve lies completely in the convex hull of the control polygon spanned by $V_0, ..., V_5$.

(5) Variation diminishing property : no straight line intersects a Bézier curve more times than it intersects its control polygon.

(6) Convexity-preserving property: the variation diminishing property means the convexity preserving property holds.

3. Trigonometric Parametric Curve Segments

Given the interpolation points $P_i,\ i = 0, 1, 2, 3$ and the trigonometric Bézier control points $V_i,\ i = 0, ..., 5$, allowing for the continuity and the shape preserving property, the terminal points requirements are given in the following:

$$\begin{cases} B_\beta(0) = V_0 \ = \ P_1, \\ B'_\beta(0) = 4(V_1 - V_0)\beta \ = \ \alpha_1(P_2 - P_0), \\ B''_\beta(0) = 12(V_0 - 2V_1 + V_2)\beta^2 \ = \ \alpha_1(P_0 - 2P_1 + P_2), \\ B''_\beta(\frac{\pi}{2\beta}) = 12(V_3 - 2V_4 + V_5)\beta^2 \ = \ \alpha_2(P_1 - 2P_2 + P_3), \\ B'_\beta(\frac{\pi}{2\beta}) = 4(V_5 - V_4)\beta \ = \ \alpha_2(P_3 - P_1), \\ B_\beta(\frac{\pi}{2\beta}) = V_5 \ = P_2, \end{cases} \tag{4}$$

where $\alpha_1, \alpha_2 \in [0, +\infty[$ are shape parameters and $\beta > 0$ is a tension parameter. We noted that these terminal points requirements are analogous to those given in [20].

The curve segment can be generated, using equations (4) and the blending functions, as follows:

Proposition 3.1 *Let β be the tension parameter, $V_i,\ i = 0, ..., 5$ the control points and $P_i,\ i = 0, 1, 2, 3$ the corresponding interpolation points, then, we have for $t \in [0, \frac{\pi}{2\beta}]$:*

$$P_\beta(t, \alpha_1, \alpha_2) = \sum_{i=0}^{5} B_{i,\beta}(t)V_i \ = \ \sum_{i=0}^{3} TB_{i,\beta}(t, \alpha_1, \alpha_2)P_i \tag{5}$$

where

$$\begin{cases} TB_{0,\beta}(t, \alpha_1, \alpha_2) = -\frac{\alpha_1}{4\beta}B_{1,\beta}(t) + \left(\frac{\alpha_1}{12\beta^2} - \frac{\alpha_1}{2\beta}\right) B_{2,\beta}(t), \\ TB_{1,\beta}(t, \alpha_1, \alpha_2) = B_{0,\beta}(t) + B_{1,\beta}(t) + \left(1 - \frac{\alpha_1}{6\beta^2}\right) B_{2,\beta}(t) + \left(\frac{\alpha_2}{12\beta^2} + \frac{\alpha_2}{2\beta}\right) B_{3,\beta}(t) + \frac{\alpha_2}{4\beta}B_{4,\beta}(t) \\ TB_{2,\beta}(t, \alpha_1, \alpha_2) = \frac{\alpha_1}{4\beta}B_{1,\beta}(t) + \left(\frac{\alpha_1}{12\beta^2} + \frac{\alpha_1}{2\beta}\right) B_{2,\beta}(t) + \left(1 - \frac{\alpha_2}{6\beta^2}\right) B_{3,\beta}(t) + B_{4,\beta}(t) + B_{5,\beta}(t) \\ TB_{3,\beta}(t, \alpha_1, \alpha_2) = \left(\frac{\alpha_2}{12\beta^2} - \frac{\alpha_2}{2\beta}\right) B_{3,\beta}(t) - \frac{\alpha_2}{4\beta}B_{4,\beta}(t). \end{cases} \tag{6}$$

Proof Let

$$\begin{cases} TB_{0,\beta}(t, \alpha_1, \alpha_2) = a_{00}B_{0,\beta}(t) + a_{01}B_{1,\beta}(t) + a_{02}B_{2,\beta}(t) + a_{03}B_{3,\beta}(t) + a_{04}B_{4,\beta}(t) + a_{05}B_{5,\beta}(t), \\ TB_{1,\beta}(t, \alpha_1, \alpha_2) = a_{10}B_{0,\beta}(t) + a_{11}B_{1,\beta}(t) + a_{12}B_{2,\beta}(t) + a_{13}B_{3,\beta}(t) + a_{14}B_{4,\beta}(t) + a_{15}B_{5,\beta}(t), \\ TB_{2,\beta}(t, \alpha_1, \alpha_2) = a_{20}B_{0,\beta}(t) + a_{21}B_{1,\beta}(t) + a_{22}B_{2,\beta}(t) + a_{23}B_{3,\beta}(t) + a_{24}B_{4,\beta}(t) + a_{25}B_{5,\beta}(t), \\ TB_{3,\beta}(t, \alpha_1, \alpha_2) = a_{30}B_{0,\beta}(t) + a_{31}B_{1,\beta}(t) + a_{32}B_{2,\beta}(t) + a_{33}B_{3,\beta}(t) + a_{34}B_{4,\beta}(t) + a_{35}B_{5,\beta}(t). \end{cases} \tag{7}$$

From (5) and (7), we have

$$\begin{aligned} \sum_{i=0}^{5} B_{i,\beta}(t)V_i = {} & (a_{00}B_{0,\beta}(t) + a_{01}B_{1,\beta}(t) + a_{02}B_{2,\beta}(t) + a_{03}B_{3,\beta}(t) + a_{04}B_{4,\beta}(t) + a_{05}B_{5,\beta}(t))\, P_0 \\ & + (a_{10}B_{0,\beta}(t) + a_{11}B_{1,\beta}(t) + a_{12}B_{2,\beta}(t) + a_{13}B_{3,\beta}(t) + a_{14}B_{4,\beta}(t) + a_{15}B_{5,\beta}(t))\, P_1 \\ & + (a_{20}B_{0,\beta}(t) + a_{21}B_{1,\beta}(t) + a_{22}B_{2,\beta}(t) + a_{23}B_{3,\beta}(t) + a_{24}B_{4,\beta}(t) + a_{25}B_{5,\beta}(t))\, P_2 \\ & + (a_{30}B_{0,\beta}(t) + a_{31}B_{1,\beta}(t) + a_{32}B_{2,\beta}(t) + a_{33}B_{3,\beta}(t) + a_{34}B_{4,\beta}(t) + a_{35}B_{5,\beta}(t))\, P_3. \end{aligned}$$

We then have

$$B_{0,\beta}(t)V_0 = B_{0,\beta}(t)\left(a_{00}P_0 + a_{10}P_1 + a_{20}P_2 + a_{30}P_3\right),$$
$$B_{1,\beta}(t)V_1 = B_{1,\beta}(t)\left(a_{01}P_0 + a_{11}P_1 + a_{21}P_2 + a_{31}P_3\right),$$
$$B_{2,\beta}(t)V_2 = B_{2,\beta}(t)\left(a_{02}P_0 + a_{12}P_1 + a_{22}P_2 + a_{32}P_3\right),$$
$$B_{3,\beta}(t)V_3 = B_{3,\beta}(t)\left(a_{03}P_0 + a_{13}P_1 + a_{23}P_2 + a_{33}P_3\right),$$
$$B_{4,\beta}(t)V_4 = B_{4,\beta}(t)\left(a_{04}P_0 + a_{14}P_1 + a_{24}P_2 + a_{34}P_3\right),$$
$$B_{5,\beta}(t)V_5 = B_{5,\beta}(t)\left(a_{05}P_0 + a_{15}P_1 + a_{25}P_2 + a_{35}P_3\right).$$

Furthermore, we have the following

$$\begin{cases} V_0 = a_{00}P_0 + a_{10}P_1 + a_{20}P_2 + a_{30}P_3, \\ V_1 = a_{01}P_0 + a_{11}P_1 + a_{21}P_2 + a_{31}P_3, \\ V_2 = a_{02}P_0 + a_{12}P_1 + a_{22}P_2 + a_{32}P_3, \\ V_3 = a_{03}P_0 + a_{13}P_1 + a_{23}P_2 + a_{33}P_3, \\ V_4 = a_{04}P_0 + a_{14}P_1 + a_{24}P_2 + a_{34}P_3, \\ V_5 = a_{05}P_0 + a_{15}P_1 + a_{25}P_2 + a_{35}P_3. \end{cases} \tag{8}$$

According to (8) and using (4), we deduce that $TB_{j,\beta}(t,\alpha_1,\alpha_2),\ j = 0,1,2,3,$ can be written in the form (6). ■

Remark 1

- The $TB_{i,\beta},\ i = 0,...,3$ verify the partition of unity : $\sum_{i=0}^{3} TB_{i,\beta}(t,\alpha_1,\alpha_2) = 1$;
- For $\beta = 1$, we find exactly the $TB_i(t,\alpha_1,\alpha_2)$ expressions described in [20].

4. Shape Preserving Interpolation Spline Curves

4.1 *Trigonometric parametric Spline Curves*

Let $P_i \in \mathbb{R}^d$ $(i = 0,...,n-1,\ d = 2,3)$ be the interpolation points, $U = (u_1,u_2,...,u_{n-1})$ the knot vector where $u_1 < u_2 < ... < u_{n-1}$ and shape parameters $\alpha_i \in [0,+\infty[$, $(i = 0,...,n-1)$.

For $i = 1,...,n-2$, the ith trigonometric parametric curve segment is given as a function of $TB_{j,\beta}(t,\alpha_i,\alpha_{i+1}),\ j = 0,...,3$, by the following expression:

$$P_{i,\beta}(t,\alpha_i,\alpha_{i+1}) = \sum_{j=0}^{3} TB_{j,\beta}(t,\alpha_i,\alpha_{i+1})P_{i+j-1}, \qquad 0 \leqslant t \leqslant \frac{\pi}{2\beta}. \tag{9}$$

The corresponding trigonometric parametric spline curve, of the studied basis, composed by all of the trigonometric parametric curve segments are defined as follows, for $i = 1,...,n-1$,

$$P_\beta(u) = P_{i,\beta}\left(\frac{\pi}{2\beta} \times \frac{u-u_i}{\Delta u_i},\alpha_i,\alpha_{i+1}\right), \qquad u \in [u_i,u_{i+1}], \tag{10}$$

where $\Delta u_i = u_{i+1} - u_i$.

As described in [20], $P_\beta(u)$ interpolates the interpolation points $P_i,\ i = 0,...,n-1$. As an example, adding two control interpolation points P_{-1}, P_{n+1}, two knots u_0, u_n, and two shape parameters α_0, α_n are sufficient to construct an open curve $P_\beta(u)$ interpolating all of the points $P_i,\ i = 0,...,n-1$. Closed Bézier curves are generated by specifying the first and the last control points at the same position. For constructing a closed curve $P_\beta(u)$ interpolating all of the points $P_i,\ i = 0, ..., n-1$, we have to add three interpolation points $P_{-1} = P_n$, $P_{n+1} = P_0$, $P_{n+2} = P_1$ three knots u_0, u_n, u_{n+1}, and three shape parameters α_0, α_n, α_{n+1}.

4.2 *Trigonometric Parametric Spline Surfaces*

A surface may be defined by the tensor product of two curves so that the properties of the blending functions are not modified. Tensor product B-spline surfaces whereas a curve requires one tension parameter for its definition, a surface requires two tension parameters $\beta > 0$ and $\lambda > 0$. Similarly to the work done by Liu et al. (see [17]), we define trigonometric parametric spline surfaces as a tensor product. More precisely we have the following definition.

Definition 4.1 *Given $m \times n$ interpolation points P_{kl} $(k = 0, 1, ..., m-1;\ l = 0, 1, ..., n-1)$, two knot vectors $U = [u_1, u_2, ..., u_{m-1}]$ and $V = [v_1, v_2, ..., v_{n-1}]$ and two shape parameters vectors $\alpha = [\alpha_1, \alpha_2, ..., \alpha_{m-1}]$ and $\mu = [\mu_1, \mu_2, ..., \mu_{n-1}]$. For tension parameters $\beta > 0$ and $\lambda > 0$, the trigonometric parametric spline surface patch has the form :*

$$S_{i,j}^{\beta,\lambda}(u, v, \alpha_i, \alpha_{i+1}, \mu_j, \mu_{j+1}) = \sum_{k=0}^{3}\sum_{l=0}^{3} TB_{k,\beta}(u, \alpha_i, \alpha_{i+1}) TB_{l,\lambda}(v, \mu_j, \mu_{j+1}) P_{i+k-1, j+l-1}, \tag{11}$$

where $u \in [0, \frac{\pi}{2\beta}]$, $v \in [0, \frac{\pi}{2\lambda}]$, $i = 0, ..., m-2$ and $j = 0, ..., n-2$.
Then the trigonometric parametric spline surface is given by,

$$S^{\beta,\lambda}(u, v) = S_{i,j}^{\beta,\lambda}\left(\frac{\pi}{2\beta} \times \frac{u - u_i}{\Delta u_i}, \frac{\pi}{2\lambda} \times \frac{v - v_j}{\Delta v_j}, \alpha_i, \alpha_{i+1}, \mu_j, \mu_{j+1}\right), \quad u \in [u_i, u_{i+1}], v \in [v_j, v_{j+1}]. \tag{12}$$

5. Numerical Examples and Application

In order to justify the accuracy and efficiency of our presented trigonometric functions we consider some graphical examples.

5.1 *Trigonometric Interpolation Spline Curves and Surfaces*

Taking into account the wide range of applications of B-spline functions, it seems that the properties of B-spline functions mentioned above can be useful in solving some problems related to approximation theory, numerical analysis or computer graphics, for example representation of splines. To compare our computed results and justify the accuracy and efficiency of our presented trigonometric functions we consider the following examples. Figures 3 and 4 show open trigonometric polynomial planar curves generated by using the shape preserving trigonometric interpolation spline curves given in this paper. The plots of the given examples, for the same control polygon, are obtained for different values of β and α. It can be seen that the space curve preserve nice feature for the space interpolation points. Figures 5, 6 and 7 show closed trigonometric polynomial curves generated by using the shape preserving trigonometric interpolation spline curves, obtained for different values of β and α. The open and closed planar curves were generated by projecting the space curve $P_\beta(u)$ into the plane. Figure 8 shows the graph control polygon and the trigonometric parametric interpolation spline surface for different values of the tension parameters β and λ.

Note that, for each illustration example we took the following : $u_i = i \times h$ with $h = \frac{\pi}{2\beta(n-3)}$, $\alpha_i = \alpha$ and $\mu_i = \mu$, $\forall\ i$. The values of α, β, λ and μ are given in the figure captions.

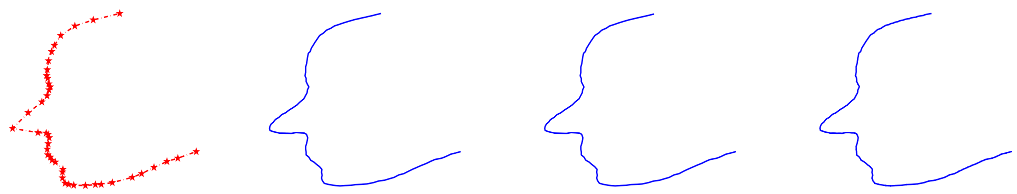

(a) Control polygon. (b) $\beta = 0.5, \alpha = 8 \times 10^{-4}$. (c) $\beta = 3\pi$, $\alpha = 8 \times 10^{-4}$. (d) $\beta = 2$, $\alpha = 10^{-2}$.

Figure 3. Open planar curves.

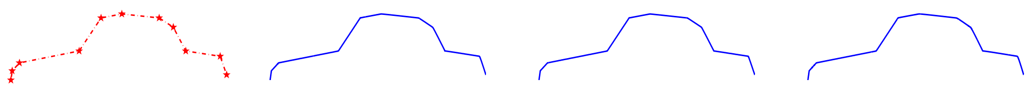

(a) Control polygon. (b) $\beta = 4, \alpha = 2 \times 10^{-2}$. (c) $\beta = 15, \alpha = 2 \times 10^{-2}$. (d) $\beta = 7, \alpha = 2 \times 10^{-2}$.

Figure 4. Open planar curves.

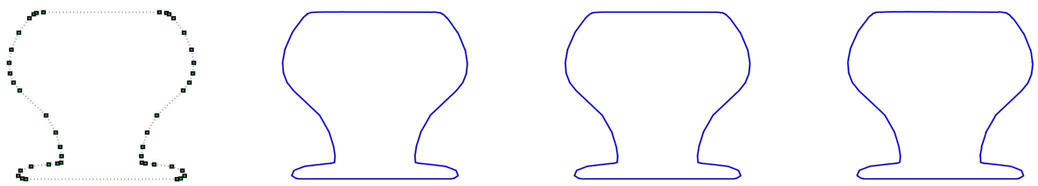

(a) Control polygon. (b) $\beta = 0.8, \alpha = 1.25 \times 10^{-2}$. (c) $\beta = 1.5, \alpha = 1.25 \times 10^{-2}$. (d) $\beta = 7, \alpha = 1.25 \times 10^{-2}$.

Figure 5. Closed planar curves.

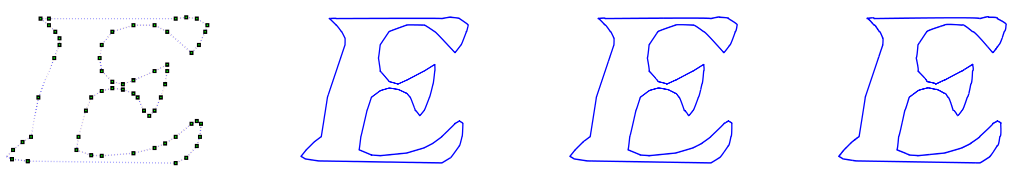

(a) Control polygon. (b) $\beta = 0.8$, $\alpha = 10^{-2}$. (c) $\beta = 1.5$, $\alpha = 10^{-2}$. (d) $\beta = \pi$, $\alpha = 10^{-2}$.

Figure 6. Closed planar curves.

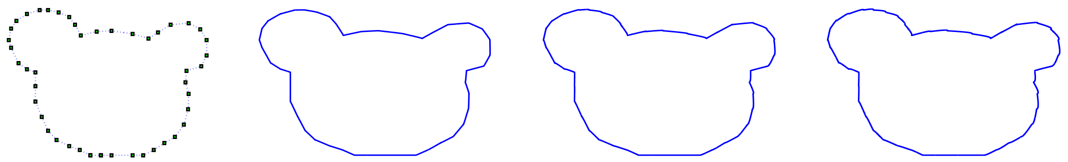

(a) Control polygon. (b) $\beta = 0.8, \alpha = 1.25 \times 10^{-2}$. (c) $\beta = 15, \alpha = 1.25 \times 10^{-2}$. (d) $\beta = 7, \alpha = 1.25 \times 10^{-2}$.

Figure 7. Closed planar curves.

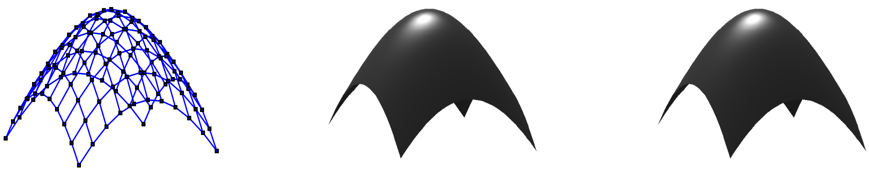

(a) Control polygon. (b) $\beta = 0.1,\ \alpha = 0.1$. (c) $\beta = 0.5,\ \alpha = 0.1$.

Figure 8. Trigonometric parametric spline surface with different values of tension parameters.

5.2 *Area of Closed Planar Curves*

In this subsection, we are interested to compute the area of closed planar curves by using Green's theorem. Let $P_\beta(u) = \sum_{i=-1}^{n+2} \varphi_{i,\beta}(u) P_i$ be a closed planar trigonometric curve, with $n+4$ interpolation points $P_i = (X_{P_i}, Y_{P_i})$.

The trigonometric polynomial blending functions $\varphi_{i,\beta}$ are given by :
for $i = 2, ..., n-1$,

$$\begin{aligned}\varphi_{i,\beta}(u) = {} & TB_{0,\beta}(\frac{\pi}{2\beta} \times \frac{u-u_i}{\Delta u}, \alpha_i, \alpha_{i+1})\mathbb{1}_{[u_i,u_{i+1}]} + TB_{1,\beta}(\frac{\pi}{2\beta} \times \frac{u-u_{i-1}}{\Delta u}, \alpha_{i-1}, \alpha_i)\mathbb{1}_{[u_{i-1},u_i]} + \\ & TB_{2,\beta}(\frac{\pi}{2\beta} \times \frac{u-u_{i-2}}{\Delta u}, \alpha_{i-2}, \alpha_{i-1})\mathbb{1}_{[u_{i-2},u_{i-1}]} + TB_{3,\beta}(\frac{\pi}{2\beta} \times \frac{u-u_{i-3}}{\Delta u}, \alpha_{i-3}, \alpha_{i-2})\mathbb{1}_{[u_{i-3},u_{i-2}]},\end{aligned}$$

with the left hand side boundary trigonometric polynomial blending functions are

$$\begin{aligned}\varphi_{-1,\beta}(u) &= TB_{0,\beta}(\frac{\pi}{2\beta} \times \frac{u-u_0}{\Delta u}, \alpha_0, \alpha_1)\mathbb{1}_{[u_0,u_1]},\\ \varphi_{0,\beta}(u) &= TB_{0,\beta}(\frac{\pi}{2\beta} \times \frac{u-u_1}{\Delta u}, \alpha_1, \alpha_2)\mathbb{1}_{[u_1,u_2]} + TB_{1,\beta}(\frac{\pi}{2\beta} \times \frac{u-u_0}{\Delta u}, \alpha_0, \alpha_1)\mathbb{1}_{[u_0,u_1]},\\ \varphi_{1,\beta}(u) &= TB_{0,\beta}(\frac{\pi}{2\beta} \times \frac{u-u_1}{\Delta u}, \alpha_2, \alpha_3)\mathbb{1}_{[u_2,u_3]} + TB_{1,\beta}(\frac{\pi}{2\beta} \times \frac{u-u_1}{\Delta u}, \alpha_1, \alpha_2)\mathbb{1}_{[u_1,u_2]} + TB_{2,\beta}(\frac{\pi}{2\beta} \times \frac{u-u_0}{\Delta u}, \alpha_0, \alpha_1)\mathbb{1}_{[u_0,u_1]},\end{aligned}$$

and the right hand side ones are given by

$$\begin{aligned}\varphi_{n,\beta}(u) &= TB_{1,\beta}(\frac{\pi}{2\beta} \times \frac{u-u_n}{\Delta u}, \alpha_n, \alpha_{n+1})\mathbb{1}_{[u_n,u_{n+1}]} + TB_{2,\beta}(\frac{\pi}{2\beta} \times \frac{u-u_{n-1}}{\Delta u}, \alpha_{n-1}, \alpha_n)\mathbb{1}_{[u_{n-1},u_n]} + \\ & \quad TB_{3,\beta}(\frac{\pi}{2\beta} \times \frac{u-u_{n-2}}{\Delta u}, \alpha_{n-2}, \alpha_{n-1})\mathbb{1}_{[u_{n-2},u_{n-1}]},\\ \varphi_{n+1,\beta}(u) &= TB_{2,\beta}(\frac{\pi}{2\beta} \times \frac{u-u_n}{\Delta u}, \alpha_n, \alpha_{n+1})\mathbb{1}_{[u_n,u_{n+1}]} + TB_{3,\beta}(\frac{\pi}{2\beta} \times \frac{u-u_{n-1}}{\Delta u}, \alpha_{n-1}, \alpha_n)\mathbb{1}_{[u_{n-1},u_n]},\\ \varphi_{n+2,\beta}(u) &= TB_{3,\beta}(\frac{\pi}{2\beta} \times \frac{u-u_n}{\Delta u}, \alpha_n, \alpha_{n+1})\mathbb{1}_{[u_n,u_{n+1}]},\end{aligned}$$

From Green's theorem (see [4, 5]), the enclosed area can be written as the bilinear form of,

$$\mathcal{A}_\beta = \frac{1}{2} \oint \left| P_\beta(u) P'_\beta(u) - P'_\beta(u) P_\beta(u) \right| du, \tag{13}$$

where $\left| P_\beta(u) P'_\beta(u) - P'_\beta(u) P_\beta(u) \right|$ denotes the cross product's determinant.

Let us denote by
$\mathcal{M} = (\mathcal{M}_{i,j})_{-1 \leqslant i,j \leqslant n+2} = (\oint \left| \varphi_{i,\beta}(u) \varphi'_{j,\beta}(u) - \varphi'_{i,\beta}(u) \varphi_{j,\beta}(u) \right| du)_{-1 \leqslant i,j \leqslant n+2}$,
$X = (X_{P_{-1}}, ..., X_{P_{n+2}})^T$ and $Y = (Y_{P_{-1}}, ..., Y_{P_{n+2}})^T$.
According to the above notations, Eq. (13) is equivalent to

$$2\mathcal{A}_\beta = X^T \mathcal{M}\, Y. \tag{14}$$

The matrix $\mathcal{M}$ has the following form:

$$\mathcal{M} = \begin{pmatrix}
0 & I_1 & I_2 & I_3 & 0 & \dots & & & & & & 0 \\
-I_1 & 0 & I_6 & I_4 & I_3 & 0 & \dots & & & & & 0 \\
-I_2 & -I_6 & 0 & I_5 & I_4 & I_3 & 0 & \dots & & & & 0 \\
-I_3 & -I_4 & -I_5 & 0 & I_5 & I_4 & I_3 & 0 & \dots & & & 0 \\
0 & -I_3 & -I_4 & -I_5 & 0 & I_5 & I_4 & I_3 & 0 & \dots & & 0 \\
 & & & \ddots & \ddots & \ddots & \ddots & \ddots & \ddots & & & \\
0 & & \dots & 0 & I_3 & I_4 & I_5 & 0 & I_5 & I_4 & I_3 & 0 \\
0 & & & \dots & 0 & -I_3 & -I_4 & -I_5 & 0 & I_5 & I_4 & I_3 \\
0 & & & & \dots & 0 & -I_3 & -I_4 & -I_5 & 0 & I_6 & I_2 \\
0 & & & & & \dots & 0 & -I_3 & -I_4 & -I_6 & 0 & I_1 \\
0 & & & & & & \dots & 0 & -I_3 & -I_2 & -I_1 & 0
\end{pmatrix}$$

where:
$I_1 = \oint (\varphi_{-1,\beta}(u)\varphi'_{0,\beta}(u) - \varphi'_{-1,\beta}(u)\varphi_{0,\beta}(u))du;$
$I_2 = \oint (\varphi_{-1,\beta}(u)\varphi'_{1,\beta}(u) - \varphi'_{-1,\beta}(u)\varphi_{1,\beta}(u))du;$
$I_3 = \oint (\varphi_{-1,\beta}(u)\varphi'_{2,\beta}(u) - \varphi'_{-1,\beta}(u)\varphi_{2,\beta}(u))du;$
$I_4 = \oint (\varphi_{0,\beta}(u)\varphi'_{2,\beta}(u) - \varphi'_{0,\beta}(u)\varphi_{2,\beta}(u))du;$
$I_5 = \oint (\varphi_{1,\beta}(u)\varphi'_{2,\beta}(u) - \varphi'_{1,\beta}(u)\varphi_{2,\beta}(u))du;$
$I_6 = \oint (\varphi_{0,\beta}(u)\varphi'_{1,\beta}(u) - \varphi'_{0,\beta}(u)\varphi_{1,\beta}(u))du.$

6. Conclusion

The trigonometric polynomial blending functions constructed in this paper have the properties analogous to those of the quintic Bernstein basis functions and the trigonometric Bézier curves are also analogous to the quintic Bézier ones. In this basis we included the tension parameter which is mainly important for object visualization. The trigonometric Bézier curves are close to the control polygon. Therefore, these trigonometric Bézier curves can preserve the shape of the control polygon. For any shape parameters satisfying the shape preserving conditions, the obtained shape preserving trigonometric interpolation spline curves are all continuous. There is no need to solve a linear system and the changes of a local shape parameter will only affect two curve segments. Numerical examples indicate that our method can be applied to generate nice features preserving space curves and surfaces. Generalizing the idea to quasi-interpolation with trigonometric spline curve and tensor product surfaces will be reported in a future paper.

References

[1] M. Amirfakhrian, *Approximation of 3D-Parametric Functions by Bicubic B-spline Functions*, International Journal of Mathematical Modelling & Computations, **2 (3)** (2012) 211–220.

[2] M. Amirfakhrian and H. Nouriani, *Interpolation by Hyperbolic B-spline Functions*, Mathematical Modelling & Computations, **1 (3)** (2011) 175–181.

[3] Q. Chen and G. Wang, *A class of Bézier-like curves*, Computer Aided Geometric Design, **20 (1)** (2003) 29–39.

[4] D. Eberly and J. Lancaster, *On gray scale image measurements, I. arc length and area*, Graphical Models and Image Processing, **53 (6)** (1991) 538–549.

[5] G. Elber, *Linearizing the area and volume constraints, Technical Report*, CIS-2000-04, (2000).

[6] O. El Khayyari and A. Lamnii, *Numerical Solutions of Second Order Boundary Value Problem by Using Hyperbolic Uniform B-Splines of Order 4*, International Journal of Mathematical Modelling & Computations, **4 (1)** (2014) 25–36.

[7] X. Han, *Cubic Trigonometric Polynomial Curves with a Shape parameter*, Computer Aided Geometric Design, **21 (6)** (2004) 535–548.

[8] X. Han, *C^2 Quadratic trigonometric polynomial curves with local bias*, Journal of Computational and Applied Math, **180 (1)** (2005) 161–172.

[9] X. Han, *Quadratic trigonometric polynomial curves with a shape parameter*, Computer Aided Geometric Design, **19 (7)** (2002) 479–502.

[10] X. Han, *Quadratic trigonometric polynomial curves concerning local control*, Applied Numerical Mathematics, **56 (1)** (2006) 105–115.

[11] F. Kui, *G^2 continuous convexity preserving cubic Bézier interpolation spline curve*, Journal of Computer-Aided Design & Computer Graphics, **6 (4)** (1994) 277–282.

[12] F. Kui and S. Xingming, *Shape preserving interpolation by quintic parametric curve*, Journal on Numerical Methods and Computer Applications, **23 (1)** (2002) 24–30.

[13] A. Lamnii and H. Mraoui, *Spline Collocation Method for Solving Boundary Value Problems*, International Journal of Mathematical Modelling & Computations, **3 (1)** (2013) 11–23.

[14] A. Lamnii and H. Mraoui, *Hierarchical Computation of Hermite Spherical Interpolant*, International Journal of Mathematical Modelling & Computations, **2 (4)** (2012) 247–259.

[15] A. Lamnii, H. Mraoui, D. Sbibih and A. Zidna, *Uniform tension algebraic trigonometric spline wavelets of class C^2 and order four*, Mathematics and Computers in Simulation, **87** (2013) 68–86.

[16] H. Liu, Lu Li and D. Zhang, *Blending of the Trigonometric Polynomial Spline Curve with Arbitrary Continuous Orders*, Journal of Information & Computational Science, **11 (1)** (2014) 45–55.

[17] H. Liu, Lu Li, D. Zhang and H. Wang, *Cubic Trigonometric Polynomial B-spline Curves and Surfaces with Shape Parameter*, Journal of Information & Computational Science, **9 (4)** (2012) 989–996.

[18] E. Mainar, J. M. Pêna and J. Sánchez-Reyes, *Shape preserving alternatives to the rational Bézier model*, Computer Aided Geometric Design, **18 (1)** (2001) 37–60.

[19] W. Wentao and W. Guozhao, *Trigonometric polynomial uniform B-spline with shape parameter*, Chinese Journal of Computers, **7** (2005) 1192–1198.

[20] Y. Zhu, X. Han and J. Han, *Quartic Trigonometric Bézier Curves and Shape Preserving Interpolation Curves*, Journal of Computational Information Systems **8 (2)** (2012) 905–914.